Available online at www.sciencedirect.com
SCIENCE DIRECT®
Icarus 166 (2003) 131–140
ICARUS
www.elsevier.com/locate/icarus

Short-lived asteroids in the 7/3 Kirkwood gap and their relationship to the Koronis and Eos families

K. Tsiganis,[a,*] H. Varvoglis,[b] and A. Morbidelli [a]

[a] *Observatoire de la Côte d'Azur–Nice, UMR 6529 Cassini, CNRS, B.P. 4229, 06304 Nice cedex 4, France*
[b] *Section of Astrophysics Astronomy & Mechanics, Department of Physics, University of Thessaloniki, 54 124 Thessaloniki, Greece*

Received 20 May 2003; revised 18 August 2003

Abstract

A population of 23 asteroids is currently observed in a very unstable region of the main belt, the 7/3 Kirkwood gap. The small size of these bodies—with the notable exception of (677) Aaltje (∼ 30 km)—as well as the computation of their dynamical lifetimes ($3 < T_D < 172$ Myr) shows that they cannot be on their primordial orbits, but were recently injected in the resonance. The distribution of inclinations appears to be bimodal, the two peaks being close to 2° and 10°. We argue that the resonant population is constantly being replenished by the slow leakage of asteroids from both the Koronis ($I \sim 2°$) and Eos ($I \sim 10°$) families, due to the drift of their semi-major axes, caused by the *Yarkovsky effect*. Assuming previously reported values for the Yarkovsky mean drift rate, we calculate the flux of family members needed to sustain the currently observed population in steady state. The number densities with respect to semi-major axis of the observed members of both families are in very good agreement with our calculations. The fact that (677) Aaltje is currently observed in the resonance is most likely an exceptional event. This asteroid should not be genetically related to any of the above families. Its size and the eccentricity of its orbit suggest that the Yarkovsky effect should have been less efficient in transporting this body to the resonance than close encounters with Ceres.

Keywords: Asteroids; Dynamics, asteroids; Families, Yarkovsky effect, celestial mechanics, resonances

1. Introduction

The 7/3 mean motion resonance with Jupiter (semi-major axis $a \approx 2.956$ AU) occurs at the location of one of the famous *Kirkwood gaps* in the distribution of asteroids. However, this gap is not completely void of asteroids, as a number of ∼ 50 bodies are currently observed within or close to the borders of the resonance. The distribution of these bodies, as a function of their *proper elements*, is shown in Fig. 1. The data are taken from the "numb.syn" catalogue of the AstDyS web service,[1] where the values of numerically computed (synthetic) proper elements (Milani and Knežević, 2003) can be found for all numbered asteroids. The 7/3-resonant population mostly consists of bodies with absolute magnitudes in the range $13 < H < 15$ which, assuming their albedos to be $0.1 < A < 0.3$, translate to diameters in the range $2 \text{ km} \leqslant D \leqslant 12$ km. Asteroid (677) Aaltje is the only "large" body observed in this region, with $H = 9.3$ and $D \sim 30$ km. The small sizes of the resonant objects suggest that they are not primordial, but should be fragments of collisionally eroded bodies. Moreover, the 7/3 resonance is a highly unstable region of the main asteroid belt. Previous numerical studies have shown that the median dynamical lifetime of objects initially placed in the resonance is ∼ 20 Myr (Gladman et al., 1997). Hereafter we use the term "dynamical lifetime" to denote the time it takes for an orbit to encounter Jupiter within $1.5r_H$, where r_H is the Hill sphere of Jupiter. After an asteroid suffers such an encounter with Jupiter, it is swiftly ejected from the main belt. Given this short time scale, the probability that the currently observed resonant objects are on their primordial orbits is effectively null. The question then is where do these bodies originate from.

From Fig. 1, one can see that two big asteroid families lie on either side of the resonance. These are the *Koronis* (with semi-major axes $a < 2.955$ AU) and *Eos* ($a > 2.955$ AU) families. The family members were identified by applying a hierarchical clustering algorithm (Zappalà et al., 1995) to the AstDys data, with a code kindly provided to us by D.

* Corresponding author.
E-mail address: tsiganis@obs-nice.fr (K. Tsiganis).
[1] http://hamilton.dm.unipi.it/cgi-bin/astdys/astibo.

0019-1035/$ – see front matter
doi:10.1016/j.icarus.2003.08.007

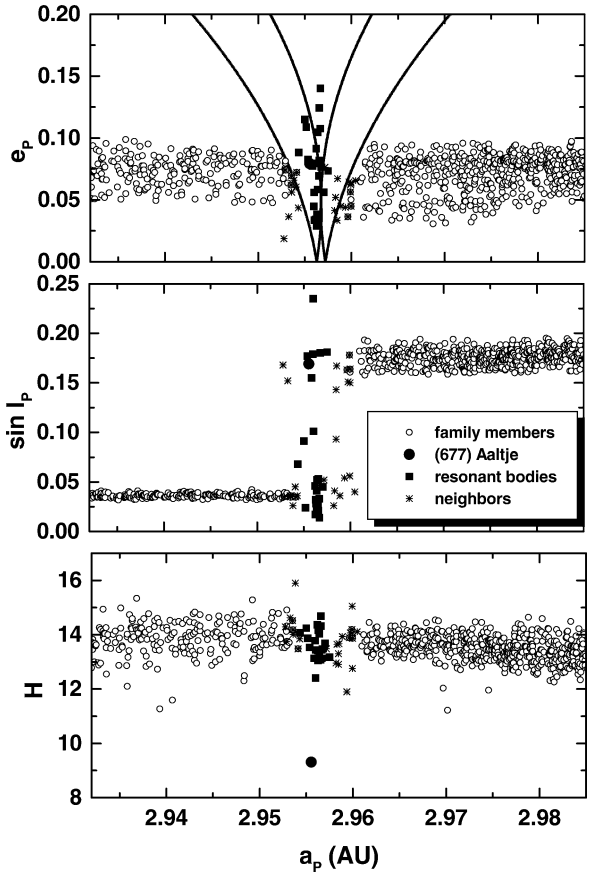

Fig. 1. (Top) The distribution of bodies in the (a, e) plane of synthetic proper elements. The data are taken from the AstDys data base. Only the objects that are dynamically affected by the $7/3$ resonance and the members of the Koronis and Eos families are shown. We distinguish between (i) objects that are currently in resonance (solid squares) and (ii) objects that are close to the borders of the resonance (stars). Asteroid (677) Aaltje—the largest resonant body—is represented by a solid circle. Finally, the open circles correspond to the members of the two families. (Middle) The same objects as in (top), projected on the $(a, \sin I)$ plane. The distinction between the low-I and high-I resonant groups is evident. (Bottom) The same objects, projected on the (a, H) plane. Both families, as well as the resonant population, have very similar magnitude distributions.

Nesvorný, and using previously reported values for the velocity cutoff, namely $v_c = 60\ \mathrm{m\,s^{-1}}$ for the Koronis and $v_c = 80\ \mathrm{m\,s^{-1}}$ for the Eos family.[2] The background population is not shown in Fig. 1, for clarity purposes.

On the (a, e) plot of Fig. 1 we have superimposed two "V"-shaped curves. These curves represent the locus of the separatrix of the $7/3$ resonance, as computed in an integrable resonance model. Let us adopt the planar elliptic three-body problem as our basic model, and denote the eccentricity of Jupiter's orbit by e'. As soon as $e' > 0$, any mean motion resonance, $(k+q)/k$, of order q (in our case $q = 7-3 = 4$) splits into a multiplet of $q+1$ closely spaced resonances. In a first approximation, the resonances are equi-spaced in mean motion space by an amount equal to the secular frequency of the perihelion, $\dot{\varpi}$, which translates to a small separation in a, say δa. For a given value of the asteroid's eccentricity, e, we can compute the width of each resonance in a, say Δa_{k}. The volume of phase space covered by chaotic trajectories and the transport properties of this set of trajectories is dictated by the ratios $\Delta a_{\mathrm{k}}/\delta a$. Using a local expansion of the disturbing function (see Murray and Dermott, 2000) and a series of canonical transformations, to express the Hamiltonian in linear proper elements (see also Murray and Holman, 1997), we found that $\Delta a_{\mathrm{k}} \gg \delta a$ for all 5 harmonics related to the $7/3$ resonance. In this case, the dynamics of the resonance are similar to those of a modulated pendulum (see Morbidelli, 2002), and the separatrix expands and contracts at a rate equal to $\langle \dot{\varpi} \rangle$. The two curves plotted in Fig. 1 represent the two extremes of the width of the $7/3$ resonance, during the modulation period. Note that, since the phase angle of the asteroids is not specified on this plot, we cannot tell which asteroid is in fact in the resonance. However, we can be sure[3] that asteroids inside the narrow "V" are in the resonance, and asteroids outside the wide "V" are not. As we can see on the plot, the Koronis and Eos families are terminated at the borders of the resonance, as these are defined by the wide separatrix. We also note that the members of both families have a distribution of absolute magnitudes, which is very similar to the one of the resonant bodies. These observational facts suggest that the two families could be the sources of the resonant population.

The genetic relationship between the resonant population and the two families is supported by the distribution of bodies in the space of proper elements. As seen in Fig. 1, all family bodies and most resonant bodies have eccentricities in the range $0.04 \leqslant e \leqslant 0.1$. A few resonant bodies have eccentricities outside this interval, but this scatter should be due to the chaotic evolution of orbits in the resonance. Even more indicative is the distribution in inclination of the resonant bodies. The projection of the asteroids on the $(a, \sin I)$ plane (I denotes the proper inclination of the asteroid's orbit) is also shown in Fig. 1. The distribution of I appears to be bimodal, the two peaks being at $I \sim 2°$ and $I \sim 10°$. These values are close to the corresponding mean values of the Koronis and the Eos family, respectively. We note that three asteroids—(8560) with $\sin I = 0.235$, (17452) with $\sin I = 0.101$ and (55501) with $\sin I = 0.091$—do not seem to obey this grouping. However we can imagine that these asteroids had in the past inclinations similar to those of the two groups mentioned above, and have slowly drifted in I, while their trajectories were evolving chaotically inside the resonance. In the following we show that this can indeed be the case.

[2] See http://www.boulder.swri.edu/~davidn/family. We note that the right-hand side of the Koronis family and the left-hand side of the Eos family are not significantly modified for $50 < v_c < 60$ and $60 < v_c < 80$ (in $\mathrm{m\,s^{-1}}$), respectively. For higher values of v_c, both families artificially cross over the $7/3$ resonance.

[3] Remember though that this is a simplified model.

Given the short dynamical lifetime of bodies in the 7/3 resonance, the presently observed objects should have been injected into the resonance quite recently (< 100 Myr). However, the ages of both the Koronis and the Eos families exceed 1 Gyr (see Marzari et al., 1999; Bottke et al., 2001; Vokrouhlický et al., 2002). Hence, the presently observed resonant bodies could not have been emplaced in the resonance immediately after the original family forming events. Therefore, we need to find a mechanism that constantly injects bodies into the 7/3 resonance, thus sustaining the resonant population in a sort of steady state. Given their small sizes, these objects suffer significant variations of their semi-major axes, due to the *Yarkovsky effect* (Farinella and Vokrouhlický, 1999). We remind the reader that the Yarkovsky effect refers to a recoil force that acts on spinning bodies as they re-emit the absorbed solar radiation.

The role played by the Yarkovsky effect in shaping the Koronis and Eos families was recently demonstrated (Bottke et al., 2001; Vokrouhlický et al., 2002). It explains the "V"-shaped distribution of members in the (a, H) plane, the footprint of a size-dependent evolution, from which a quite accurate estimate of the family ages can be deduced. Also, it explains asymmetries produced in the (a, e, I) distribution, as family members are forced to cross high-order resonances. Given these results, the Yarkovsky effect seems to be the most promising mechanism for explaining the presently observed population of 7/3-resonant bodies.

The long-term dynamics of orbits in the 7/3 resonance are studied in Section 2. As expected, the real bodies have short dynamical lifetimes. An analysis of a large set of fictitious resonant particles shows that, for inclinations similar to those of the two families, the resonance has a vanishingly small zone of stable librations. The long-term dynamics of two sets of fictitious objects, representing bodies that were injected into the resonance with Koronis-like or Eos-like eccentricities and inclinations, are also studied. The results confirm the short dynamical lifetimes found for the real resonant asteroids. In Section 3 we show that the diurnal Yarkovsky effect could provide a flux of family members that would be enough to keep the observed resonant population in steady state. Our conclusions are given in Section 4.

2. Dynamics in the 7/3 resonance

2.1. The observed population

Using the AstDys data, we selected a set of ~ 400 objects in the vicinity of the 7/3 resonance (with 2.92 AU $\leqslant a \leqslant$ 2.99 AU) and performed a numerical integration of their orbits, for a time span corresponding to 200,000 years. All our integrations were performed using the symplectic integrator of Wisdom and Holman (1991), as it is implemented in the SWIFT package (Levison and Duncan, 1994). The model accounted for the gravitational perturbations exerted by the four giant planets. The resonant asteroids were identified by inspecting the behavior of the critical argument of the 7/3 resonance, $\sigma = 7\lambda' - 3\lambda - 4\varpi$ (λ is the mean longitude and ϖ the longitude of perihelion of the asteroid; primed elements refer to Jupiter). We remind the reader that if σ is a slow angle, whose behavior changes erratically from libration to circulation, then the orbit is inside the stochastic layer of the resonance. On the other hand, if σ is a fastly circulating angle, the orbit is out of the resonance zone. We found that 23 bodies (including (677) Aaltje) are presently in the resonance, while 26 bodies are close to the borders of the resonance (see Fig. 1), since σ circulates, but not very fast. Note that all 23 resonant asteroids follow chaotic orbits, a property also reported in the AstDys catalogue, and no permanent librators were found. For all these orbits σ is changing erratically from libration to circulation, and the changes are correlated with the variations of the semi-major axis, a. This behavior, for the orbit of (677) Aaltje, can be seen in Fig. 2. As one can see in Fig. 2 there are two basic time scales governing the evolution of σ. This is a consequence of the modulated pendulum-like dynamics mentioned before. The long-periodic variations of σ are related to the evolution of ϖ and reflect a displacement of the center of libration. The short-periodic, small-amplitude, variations of σ, which correlate with the variations of a, are related to librations about the instantaneous equilibrium.

We integrated the orbits of the 23 resonant and 20 neighboring objects for 100 Myr. We excluded neighboring orbits that seem to follow stable orbits. The reason for following the orbits of the neighboring objects is to examine the diffusive region around the 7/3 resonance. Experience shows that orbits starting very close to a resonance can later on fall into the resonance, due to slow chaotic diffusion (see Guillens et al., 2002).

In this run, 20 out of the 23 resonant bodies, as well as 11 neighboring ones, encountered Jupiter before the end of the integration time. The integration continued for the remaining 3 resonant bodies, which also escaped within 172 Myr. The dynamical lifetimes of these asteroids are given in Tables 1 and 2. As was expected, the 7/3 resonance pumps the eccentricities of their orbits up to Jupiter-crossing values (~ 0.7). The typical dynamical behavior of resonant particles can be seen in Fig. 3. Both e and i undergo slow chaotic diffusion, up to a point when the orbit enters into a highly unstable region. A phase of large secular oscillations of the eccentricity follows, until the asteroid suffers a close encounter with Jupiter, which extracts it from the main belt. The median dynamical lifetime of this population is 19.3 Myr, i.e., the same as the one found by Gladman et al. (1997), while the mean value is 38.4 Myr.[4]

[4] The median dynamical lifetime is the time needed for 50% of the population to escape, while the mean dynamical lifetime is the arithmetic mean, i.e., $\sum_i T_{\mathrm{D},i}/N$, where N the total number of particles and $i = 1, \ldots, N$.

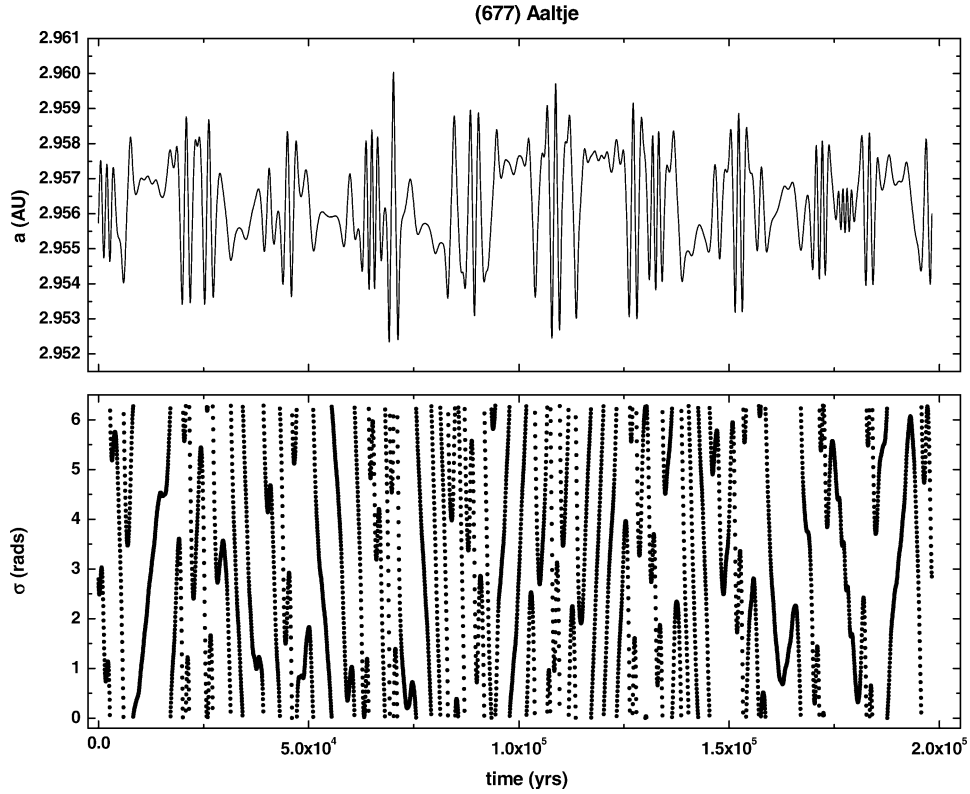

Fig. 2. Time evolution of the critical argument, σ, and the semi-major axis, a, of (677) Aaltje. The behavior of σ suggests that the motion is chaotic and that the 7/3 resonance is responsible for this chaos. The variations of a about the value $a_{\rm res} = 2.9556$ AU are correlated with the variations of σ.

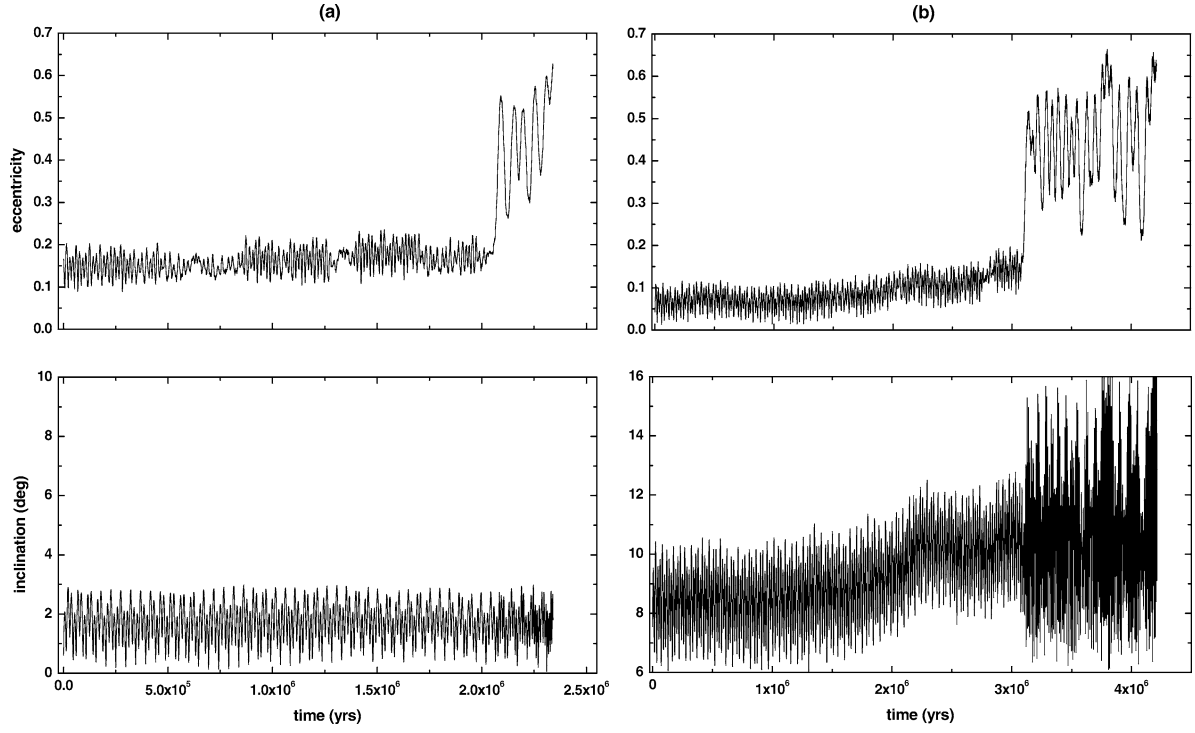

Fig. 3. Time evolution of e and i for 7/3-resonant orbits. (a) A Koronis-like particle, and (b) an Eos-like particle. The values of both elements undergo slow diffusion, until the orbit enters a "fast" chaotic path; the eccentricity then quickly increases to ~ 0.7 and the asteroid suffers a close encounter with Jupiter, which ejects it from the resonance. For Eos-like particles, the inclination also changes by large amounts, once the particle has entered the unstable region.

Table 1
Orbital and physical properties of the resonant asteroids studied in this paper

Number	a_P	e_P	$\sin I_P$	H	T_D (Myr)
(677)	2.956	0.080	0.169	9.3	7.7
(7400)	2.956	0.069	0.028	13.1	19.3
(8119)	2.956	0.140	0.014	13.1	2.4
(8422)	2.956	0.108	0.033	13.4	8.0
(8560)	2.956	0.056	0.235	12.4	10.9
(13309)	2.957	0.073	0.181	13.2	12.9
(15459)	2.955	0.109	0.024	13.9	12.8
(17452)	2.956	0.034	0.101	13.4	21.3
(19626)	2.956	0.058	0.041	13.3	26.9
(22001)	2.956	0.091	0.017	13.4	8.0
(23041)	2.954	0.088	0.068	14.1	26.2
(23777)	2.956	0.077	0.180	13.5	4.9
(24450)	2.956	0.105	0.023	14.0	11.5
(25259)	2.956	0.038	0.028	14.2	172.0
(26541)	2.956	0.029	0.032	13.1	47.8
(26584)	2.956	0.077	0.155	13.1	4.2
(28832)	2.956	0.082	0.053	14.3	83.9
(31253)	2.956	0.079	0.052	14.1	152.2
(36688)	2.956	0.034	0.046	14.4	33.3
(43575)	2.956	0.045	0.179	13.8	141.2
(46728)	2.955	0.083	0.177	13.5	7.9
(50877)	2.957	0.056	0.045	13.7	42.8
(55501)	2.955	0.115	0.091	14.2	24.1

The asteroid's designation, proper elements (a, e, and I), the absolute magnitude, H, and the dynamical lifetime of its orbit are shown.

Table 2
The same as in Table 1, but for the neighboring asteroids

Number	a_P	e_P	$\sin I_P$	H	T_D (Myr)
(16354)	2.958	0.052	0.041	13.7	53.4
(18470)	2.954	0.072	0.035	13.5	9.4
(31082)	2.959	0.067	0.167	13.7	13.3
(32603)	2.960	0.036	0.163	13.9	46.4
(32675)	2.957	0.124	0.021	14.7	71.1
(38432)	2.960	0.045	0.164	13.9	27.2
(40090)	2.960	0.056	0.178	14.2	23.7
(40986)	2.960	0.064	0.151	14.1	12.2
(43146)	2.960	0.064	0.150	12.8	36.3
(45616)	2.954	0.060	0.045	14.1	57.6
(51976)	2.957	0.076	0.052	13.5	7.9
(4258)	2.959	0.044	0.054	11.9	
(4441)	2.958	0.042	0.026	13.0	
(23538)	2.959	0.045	0.036	13.9	
(25627)	2.958	0.034	0.093	12.9	
(25768)	2.954	0.069	0.035	14.2	
(30488)	2.953	0.074	0.035	13.8	
(32660)	2.954	0.062	0.036	14.5	
(35612)	2.954	0.056	0.036	14.0	
(38557)	2.960	0.065	0.040	14.1	
(40703)	2.953	0.019	0.168	14.3	
(40810)	2.960	0.062	0.056	15.1	
(43713)	2.953	0.036	0.152	14.6	
(50878)	2.954	0.044	0.036	13.9	
(52031)	2.954	0.066	0.026	15.9	
(52531)	2.958	0.033	0.143	13.3	

The ones below the line, did not escape within 100 Myr but were not integrated for longer time.

2.2. Stability of resonant orbits

A numerical exploration of the dynamics in the 7/3 resonance was made for the two proper inclination values mentioned before, namely $I = 2^\circ$ and $I = 10^\circ$. Our initial conditions covered a region of osculating elements around the center of the resonance. However, we performed a small trick in order to be able to make comparisons with the distribution of the real asteroids in the space of proper elements. We set initially $\Omega = \Omega'$ and $i_0 = i'_0 + I$, where Ω denotes the longitude of the node, i_0 the initial value of the osculating inclination, I the desired value of the proper inclination and primed elements refer to Jupiter. Also, the argument of perihelion, ω, and the mean anomaly, M, were chosen by setting $\varpi = \varpi'$ and $\sigma = \pi$. This value of σ corresponds to the center of libration of the 7/3 resonance. The initial value of the osculating eccentricity was given by $e_0 = e + e_f$, where $e_f \approx 0.035$ is the forced eccentricity at the location of the 7/3 resonance, in the framework of the three-body problem, and e is the desired value of the proper eccentricity. For each value of I a set of 620 orbits was chosen, placed on a 31×20 grid in the (a, e) plane, with $2.943 \leqslant a \leqslant 2.968$ and $0 \leqslant e \leqslant 0.22$. Of course, the values of e and I are only approximations of the real proper values of the resulting orbits. As a test, we performed more runs, changing the initial values of e and I by small amounts, but the global stability portrait of the resonance was practically unchanged.

The variational equations were integrated for $t_{\rm int} =$ 1 Myr, in order to compute the values of the maximal Lyapunov exponent, γ, i.e., the asymptotic mean rate of exponential divergence of initially near-by orbits (Oseledec, 1968, see also Lichtenberg and Lieberman, 1983). We remind the reader that positive values of γ indicate chaotic motion, while $\gamma \sim 0$ implies regular motion. The equations were solved using the swift_lyap2 driver of the SWIFT package, which does not apply a periodic renormalization of the displacement vector. This code is appropriate for problems in which there are no close encounters, as in our case. As a test we computed γ for the 23 resonant asteroids and the resulting values are in close agreement with the ones given in the AstDys database. The solution of the variational equations, more specifically the norm of the displacement vector $d(t)$, was recorded every 1000 years, and the value of γ was obtained by performing a linear least-squares fit on $\ln[d(t)/d(0)]$. In principle, the computation of the γ requires infinite time. However, an integration time span of $\sim 10 \cdot \gamma^{-1}$ is enough for an accurate determination. The 23 resonant objects have Lyapunov times $T_L = \gamma^{-1} \sim 10000$ years. This value of T_L is of the order of the secular period of ϖ, a result typical for a resonance with the dynamics of a modulated pendulum. Thus, the time span chosen for this experiment is $\sim 100 \cdot T_L$. As we move further outside the resonance zone, the computation yields $T_L \sim t_{\rm int}$, which should not be taken as a positive indication for chaotic motion. In fact, the correlation coefficient, which measures the quality of the least squares fit, drops from 90–99% (for chaotic or-

bits) to $< 30\%$, as the oscillations of $d(t)$ dominate over any nearly zero-slope linear trend. This is also the reason why, for some orbits, we get $T_{\rm L} > t_{\rm int}$.

Figure 4 shows a graphical representation of the results. The value of the logarithm of $T_{\rm L}$ (in years) is coded on a grey-scale map, according to the scale shown in the figure. Evidently, the resonance is globally chaotic, the values of $T_{\rm L}$ being quite small. The "V"-shaped white region, in which the orbits have 10^3 yr $\leqslant T_{\rm L} \leqslant 10^4$ yr, almost coincides with the separatrix-swept zone, as the latter is predicted by the modulated pendulum approximation. Note that no stability region appears to exist around the center of the resonance, at least at this resolution. This fact argues against the possibility that the resonant bodies were "trapped" for billions of years in some stable region inside the resonance, from which they have slowly diffused away. The value of $T_{\rm L}$ increases, as the resonance center is approached, but all orbits around it are still chaotic, with $T_{\rm L} \leqslant 4 \times 10^4$ yr. This result holds for both values of I. A notable difference between the two plots is that, for $I = 10^\circ$, the small-eccentricity re-

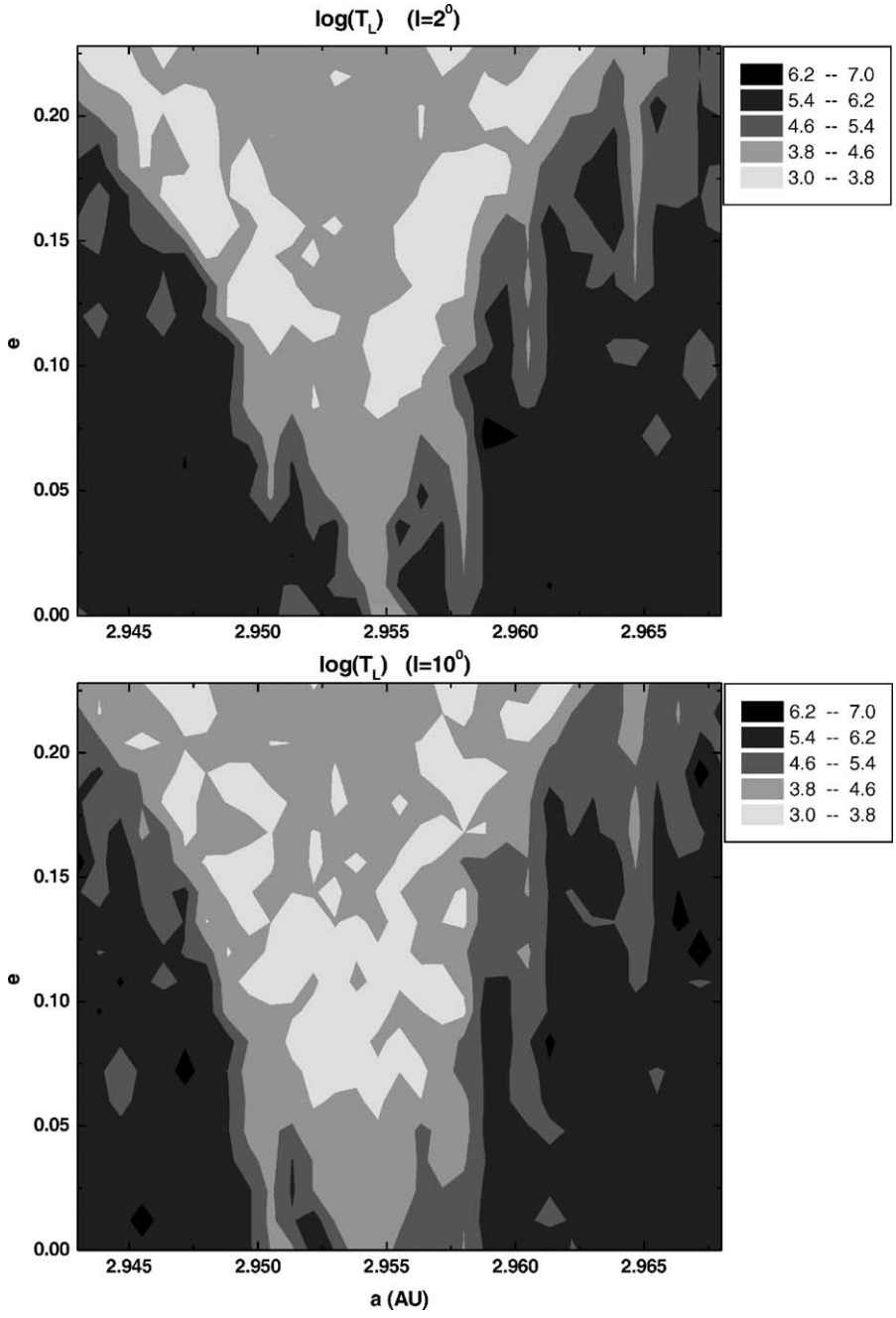

Fig. 4. Grey-scale maps of $\log(T_{\rm L})$, for $I = 2^\circ$ (top) and $I = 10^\circ$ (bottom). The scale is shown on the plot. The resonance appears to be globally chaotic and no region of stable librations is visible, at this resolution. The most chaotic region (white), associated with the separatrix-swept zone, appears to be larger for $I = 10^\circ$, extending to all values of e in the range 0.04–0.1.

gion of the resonance ($0.05 \leqslant e \leqslant 0.15$) is more chaotic than for $I = 2°$. This suggests that small-eccentricity orbits with Eos-like inclinations should reach the high-eccentricity region faster than asteroids with Koronis-like inclinations.

2.3. Long-term evolution for $I = 2°$ and $I = 10°$

Two sets, of 84 resonant particles each, were selected to study the dynamical behavior of fictitious resonant "members" of the Koronis and Eos families. Both sets of particles had initial proper eccentricities in the range $0.04 \leqslant e \leqslant 0.10$ (as before, $e_0 = e_f + e$) and semi-major axes in the range 2.9535 AU $\leqslant a \leqslant$ 2.9555 AU. The proper inclinations were selected in the range $1°.5 \leqslant I \leqslant 2°.5$ for Koronis-like objects and $9° \leqslant I \leqslant 11°$ for Eos-like objects (again, $i_0 = i'_0 + I$). The initial values for the rest of the angles were chosen in the same way as in the previous run.

The orbits of these two sets of particles were integrated until they encountered Jupiter within $1.5r_H$. Figure 5 shows the results of this experiment. Both populations decayed fast and all particles escaped within 340 Myr. We note that the decay of both groups is very well fitted by an exponential law and no tail of long-lived objects appears to exist. Along with the result shown in Fig. 4, this also suggests that the measure of the set of regular resonant orbits is negligible. If this was not the case, small "island" chains surrounded by the "ghosts" of invariant sets (cantori) would inhibit transport, leading to non-diffusive behavior (see Metzler and Klafter, 2000) and a long-lived tail. Eos-like particles escaped much faster than the Koronis-like ones, a behavior consistent with the results shown in Fig. 4. The mean dynamical lifetime for Koronis-like objects is $\langle T_D \rangle = 52.8$ Myr, while for Eos-like objects $\langle T_D \rangle = 12.4$ Myr. We note that all escaping orbits show the same evolution of e, i.e., the one already described in the case of the observed resonant bodies (see Fig. 3).

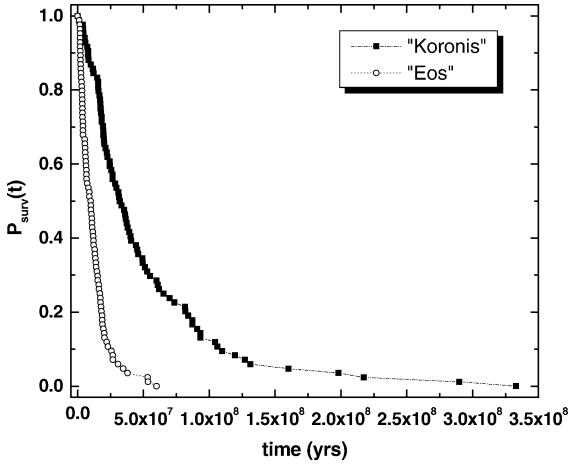

Fig. 5. The survival probability, $P_{\mathrm{surv}(t)}$, as a function of time, for the two sets of Koronis-like and Eos-like particles, placed in the 7/3 resonance. P_{surv} decays exponentially with time, for both populations. The corresponding mean values of dynamical lifetime are shown on the plot.

As stated in Section 1, we assume that all resonance bodies initially had inclinations either $I = 2°$ or $I = 10°$. Eos-like particles can actually reach inclinations as high as 16°, as seen in Fig. 3. Moreover, 24% of the Koronis-like fictitious resonant particles reach $\langle \sin I \rangle = 0.1$, as the eccentricity increases, and spend 2–20 Myr in this state, before they escape. An example of this is shown in Fig. 6. Thus, inclinations similar to those of asteroids (17452) and (55501) can be reached by chaotic diffusion inside the resonance. These results justify our initial two-group classification.

In the beginning of this section we stated that our choice of initial conditions only approximates the desired proper values of e and I. However, the two groups of fictitious particles accurately represent the evolution of the real population, on a statistical level. If we use the values of $\langle T_D \rangle$ obtained in this section, we can compute the weighed average of T_D over both inclination groups. The weighing factors are the number of observed bodies in each inclination group. The resulting weighed average of T_D has a value of 40.5 Myr, which is very close to the value obtained in Section 2.1 (38.4 Myr) from integrating the 23 resonant bodies.

3. The Yarkovsky drift of family members

Excluding (677) Aaltje, the small-inclination group of the resonant population contains $N = 16$ bodies, while the large-inclination group contains $N = 6$ bodies. Given the values of $\langle T_D \rangle$ computed above, the flux of bodies from each family, needed to keep the observed populations of resonant objects in steady state, is

$$F_{ss} = \frac{N}{\langle T_D \rangle}, \tag{1}$$

i.e., 0.48 and 0.30 bodies per Myr, for members of the Koronis and the Eos family, respectively. The question now is whether the Yarkovsky effect can match this flux.

The mean drift rate of the semi-major axis of $D = 1$ km-bodies due to the Yarkovsky effect is $\langle \Delta a \rangle / t = 1/\tau = 2.7 \times 10^{-4}$ AU Myr^{-1}. For $D > 1$ km, the drift rate is approximately inversely proportional to D (Farinella and Vokrouhlický, 1999). Assuming that Koronis-like resonant bodies (i.e., $I \sim 2°$) have the same albedo as Koronis itself ($A = 0.28$) and Eos-like bodies ($I \sim 10°$) the albedo of Eos ($A = 0.14$), the mean diameters of the currently observed resonant groups are 4.6 and 6.4 km, respectively. Therefore, $\tau^{-1} = 5.87 \times 10^{-5}$ AU Myr^{-1} and 4.22×10^{-5} AU Myr^{-1}, respectively. These numbers are computed, assuming that the obliquity of the asteroid's spin axis, θ, is either 0° or 180°. For the Koronis family, there are observational evidence that this is indeed the case (Slivan, 2002). On the other hand, assuming random obliquities in the $[0, \pi]$ interval, the above mentioned drift rate should be multiplied by $\langle (\cos\theta)^2 \rangle = \pi/4 \approx 0.785$.

The mean time, required for an asteroid to drift in semi-major axis by δa, is $\langle T_{\mathrm{drift}} \rangle = \delta a \cdot \tau$ Myr. Denoting by $N(\delta a)$

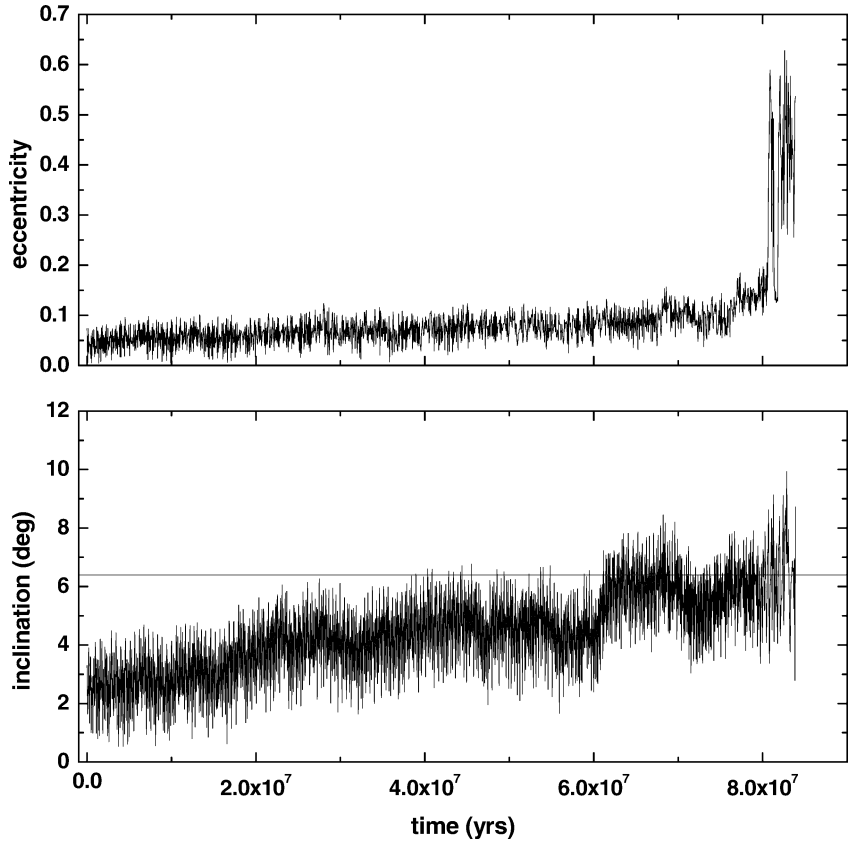

Fig. 6. Time evolution of e and i for a Koronis-like fictitious particle. Note that the inclination can reach a mean value of $\langle i \rangle = 6^\circ.5$, about 20 Myr before the eccentricity starts to undergo wild oscillations. 24% of Koronis-like particles follow similar evolution.

the number of bodies within a distance δa from the border of the resonance, the mean flux into the resonance is

$$F_\pm = \frac{N(\delta a)}{2\,\langle T_{\rm drift}\rangle}, \tag{2}$$

where the factor 2 in the denominator is due to the fact that asteroids can drift towards smaller or larger values of a with the same probability. Since we ask for the steady state solution, we impose $F_\pm = F_{\rm SS}$ and solve for $N(\delta a)$. The result is that, to explain the observed resonant group at $I \sim 2^\circ$, 19–24 bodies per 0.002 AU should be currently observed in the Koronis family. Similarly, for the $I \sim 10^\circ$ group, we should be observing 45–57 bodies per 0.002 AU in the Eos family. The lower bounds of these estimates correspond to θ being either 0° or 180°, while the upper bounds are computed for randomized values of θ. The results are summarized in Table 3.

The above calculations are true, if we consider only the *diurnal* and not the *seasonal* variant of the Yarkovsky effect, the latter leading to a secular drift of a towards smaller values. However, the seasonal effect is much weaker than the diurnal one, especially for obliquities much different than 90°. Thus, for time scales comparable to the ones dictated by the dynamics in the 7/3 resonance, we can neglect the seasonal effect in an order of magnitude estimate of the drift rate.

Table 3
Replenishment of the 7/3-resonant groups by the Koronis and Eos families, due to the Yarkovsky effect

Group	$N_{\rm obs}$	$\langle D \rangle$ (km)	$\langle T_{\rm D} \rangle$ (Myr)	$F_{\rm ss}$ (Myr^{-1})	$N_{\rm Yar}(\delta a)$
$I \sim 2^\circ$	16	4.6	52.8	0.48	19–24 (Koronis)
$I \sim 10^\circ$	6	6.4	12.4	0.30	45–57 (Eos)

The two resonant groups are labeled by their typical value of I. $N_{\rm obs}$ denotes the number of bodies that are currently observed in each group, and the next column gives their mean diameter, for an albedo equal to that of (158) Koronis or (221) Eos, respectively. The next two columns give the mean dynamical lifetime of Koronis-like and Eos-like particles injected into resonance, and the flux needed to keep the observed population in steady state. The final column gives the number of family members per $\delta a = 0.002$ AU that should be observed, in order for the Yarkovsky flux, $F_\pm$, to be equal to the steady state value.

Figure 6 shows the observed distribution of the members of the Koronis and Eos families in a, binned to 0.002 AU. The horizontal lines mark the estimates we arrived at by calculating the drift due to the Yarkovsky effect. As we can see, the agreement between the number density of observed asteroids away from the nominal resonance location $a_{\rm res}$, on one hand, and the number density calculated above, on the other, is very good. However, while the number density of family members is almost constant away from the resonance, it drops significantly as the resonance borders are

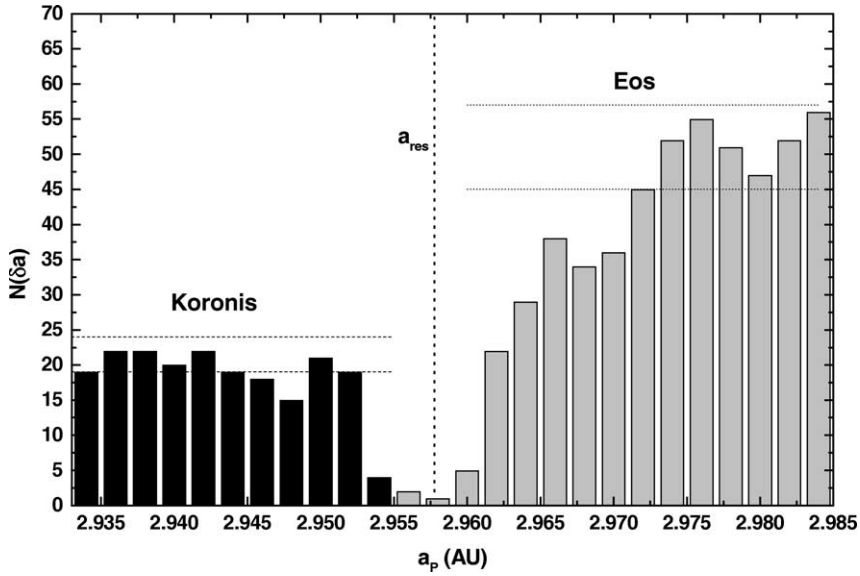

Fig. 7. Histogram of the number of observed members of the Koronis and Eos families, binned to 0.002 AU. The Koronis family has ~ 20 members per bin, while the Eos family has ~ 50 members per bin. These numbers decrease as the separatrix of the resonance is approached. The horizontal lines mark the values needed for the Yarkovsky flux to keep the observed bimodal resonant population in a steady state. The agreement between the observed and the calculated values shows that the Yarkovsky effect is responsible for replenishing the 7/3 resonance such that, at any time, the resonance contains approximately (i) the same number of resonant bodies as currently observed and (ii) the same number of asteroids in each of the two currently observed inclination groups.

approached. This is a consequence of the fact that the motion in the vicinity of the resonance borders is also chaotic. Consequently, asteroids within ~ 0.015 AU from the resonance borders tend to slowly migrate in proper elements space (chaotic diffusion), falling into the resonance on a timescale shorter than the one dictated by the Yarkovsky drift time, $\langle T_{\rm drift} \rangle$. This was shown by Guillens et al. (2002) for objects in the vicinity of the 3/1 resonance. In our case, we find an observational asymmetry, i.e., chaotic diffusion is more important for Eos members than for Koronis members. This agrees with our results on the degree of chaos in the 7/3 resonance as a function of the inclination, presented above (see Fig. 4). In this framework, if we want to correctly evaluate the number of asteroids supplied by the Yarkovsky effect to the resonance, we need to measure the flux of asteroids into the region characterized by chaotic diffusion, and not the flux into the resonance itself. For this reason, we should "shift" the boundaries of the resonance by ~ 0.015 AU away from the nominal resonance borders. In doing this we implicitely assume that all bodies entering the diffusive neighborhood will eventually fall into the resonance, neglecting the possibility of their collisional disruption in the diffusion zone. This should not be a severe simplification, given that the typical collisional lifetime for $D > 1$ km bodies is $T_{\rm col} > 350$ Myr. (See Fig. 7.)

Note that, throughout this paragraph, we have compared the population of *observed* resonant bodies, with the *observed* family members. This avoids problems coming from possible observation biases. Since the region we study has a total width of only 0.05 AU and the absolute magnitudes of all objects are in the same range ($12 < H < 15$, see Fig. 1), the population of both the resonance zone as well as of the neighboring families should be biased in the same way.

4. Conclusions

The small sizes and short dynamical lifetime of the bodies in the 7/3 resonance suggest that this population is not primordial. These asteroids should have been injected into the resonance quite recently. The two major candidate sources of these bodies are the Koronis and Eos families. As these two families have ages that exceed 1 Gyr (Marzari et al., 1999; Bottke et al., 2001; Vokrouhlický et al., 2002), the currently observed resonant bodies could not have been placed in the resonance at the epochs of the original family formation events.

We investigated the idea that the resonant population is constantly being replenished by the members of the two families, through a constant drift in semi-major axis caused by the Yarkovsky effect. We calculated the flux of bodies resulting from this drift and our computations show that the number of observed family members in the vicinity of the resonance is in very good agreement with the one needed to keep the currently observed resonant population in steady state. Unfortunately, apart from (677) Aaltje, the spectral properties of the resonant objects are not known at present, so we cannot compare them to those of (158) Koronis and (221) Eos.

Up to this point we have excluded (677) Aaltje from our study. The reason is that this object is unlikely to be related with the considered families. In fact, because of its large size, the Yarkovsky effect could not have moved this body more

than 0.01 AU over the lifetime of the Solar System, but family members of comparable size are much further from the 7/3 resonance than this amount. Moreover, this body, despite belonging to the high-inclination group of the resonant population (the one supposedly of Eos-family origin), it has a spectral type (Sl) that is different from that of (221) Eos (K) (see Bus and Binzel, 2002). As a plausible scenario explaining the presence of (677) Aaltje in the 7/3 resonance, we note that its orbit leads to close approaches with Ceres. According to Nesvorný et al. (2002), the mean change of semi-major axis, due to close encounters with Ceres, is almost an order of magnitude greater than the change due to the Yarkovsky effect, for an object of this size. Moreover, Carruba et al. (2003) have shown that encounters with Ceres are very effective (in terms of Δa) for objects located between the 5/2 and 7/3 mean motion resonances, with $e \sim 0.1$–0.15 and $I \sim 15°$. Given these results, we think that encounters with Ceres are more likely to have transported (677) Aaltje into the resonance, than the Yarkovsky effect. In any case, the fact that there is no significant source of ~ 30 km bodies within 0.1 AU from the 7/3 resonance, makes us think that the current presence of a body of this size in the 7/3 resonance is an exceptional event.

Acknowledgments

We thank Hans Scholl, Fernando Roig, and an anonymous referee for a critical reading of the first version of this paper and a series of comments that improved the presentation of this work. The work of K. Tsiganis is supported by an EU Marie Curie Individual Fellowship, under contract No. HPMF-CT-2002-01972.

References

Bottke, W.F., Vokrouhlický, D., Broz, M., Nesvorný, D., Morbidelli, A., 2001. Dynamical spreading of asteroid families by the Yarkovsky effect. Science 294, 1693–1696.

Bus, S.J., Binzel, R.P., 2002. Phase II of the small main-belt asteroid spectroscopic survey. A feature-based taxonomy. Icarus 158, 146–177.

Carruba, V., Burns, J.A., Bottke, W., Nesvorný, D., 2003. Orbital evolution of the Gefion and Adeona asteroid families: close encounters with massive asteroids and the Yarkovsky effect. Icarus 162, 308–327.

Farinella, P., Vokrouhlický, D., 1999. Semi-major axis mobility of asteroid fragments. Science 283, 1507–1510.

Gladman, B., Migliorini, F., Morbidelli, A., Zappalà, V., Michel, P., Cellino, A., Froeschlé, C., Levison, H.F., Bailey, M., Duncan, M., 1997. Dynamical lifetimes of objects injected into asteroid belt resonances. Science 277, 197–201.

Guillens, S.A., Vieira Martins, R., Gomes, R.S., 2002. A global study of the 3 : 1 resonance neighborhood: a search for unstable asteroids. Astron. J. 124, 2322–2331.

Levison, H.F., Duncan, M., 1994. The long-term dynamical behavior of short-period comets. Icarus 108, 18–36.

Lichtenberg, A.J., Lieberman, M.A., 1983. Regular and Stochastic Motion. Springer-Verlag, New York.

Marzari, F., Farinella, P., Davis, D.R., 1999. Origin, aging, and death of asteroid families. Icarus 142, 63–77.

Metzler, R., Klafter, J., 2000. The random walk's guide to anomalous diffusion: a fractional dynamics approach. Phys. Rep. 339, 1–77.

Milani, A., Knežević, Z., 2003. The determination of asteroid proper elements. In: Bottke, W.F., Cellino, A., Paolichi, P., Binzel, R.P. (Eds.), Asteroids III. Univ. of Arizona Press, Tucson, pp. 603–612.

Morbidelli, A., 2002. Modern Celestial Mechanics: Aspects of Solar System Dynamics. Taylor & Francis, London.

Murray, C.D., Dermott, S.F., 2000. Solar System Dynamics. Cambridge Univ. Press, Cambridge, UK.

Murray, N., Holman, M., 1997. Diffusive chaos in the outer asteroid belt. Astron. J. 114, 1246–1259.

Nesvorný, D., Morbidelli, A., Vokrouhlický, D., Bottke, W.F., Broz, M., 2002. The Flora family: a case of the dynamically dispersed collisional swarm? Icarus 157, 155–172.

Oseledec, V.I., 1968. The multiplicative ergodic theorem: the Lyapunov characteristic numbers of dynamical systems. Trans. Mosc. Soc. 19, 197.

Slivan, S.M., 2002. Spin vector alignment of Koronis family asteroids. Nature 419, 49–51.

Vokrouhlický, D., Broz, M., Morbidelli, A., Bottke, W.F., Nesvorný, D., Lazzaro, D., Rivkin, A.S., 2002. Yarkovsky footprints in the Eos family. In: Asteroids, Comets, Meteors, p. 115. Abstracts Book.

Wisdom, J., Holman, M., 1991. Symplectic maps for the N-body problem. Astron. J. 102, 1528–1538.

Zappalà, V., Bendjoya, Ph., Cellino, A., Farinella, P., Froeschlé, C., 1995. Asteroid families: search of a 12,487-asteroid sample using two different clustering techniques. Icarus 116, 291–314.